AAC
Journals.ASM.org

VraSR Two-Component Regulatory System Contributes to *mprF*-Mediated Decreased Susceptibility to Daptomycin in *In Vivo*-Selected Clinical Strains of Methicillin-Resistant *Staphylococcus aureus*

Shrenik Mehta,[a] Arabela X. Cuirolo,[a] Konrad B. Plata,[b] Sarah Riosa,[b] Jared A. Silverman,[c] Aileen Rubio,[c] Roberto R. Rosato,[b] and Adriana E. Rosato[b]

Division of Infectious Diseases, Department of Internal Medicine, Virginia Commonwealth University, Richmond, Virginia, USA[a]; Department of Pathology and Genomic Medicine, Center for Molecular and Translational Human Infectious Diseases Research, The Methodist Hospital Research Institute, Houston, Texas, USA[b]; and Cubist Pharmaceuticals, Lexington, Massachusetts, USA[c]

Daptomycin (DAP) is a new class of cyclic lipopeptide antibiotic highly active against methicillin-resistant *Staphylococcus aureus* (MRSA) infections. Proposed mechanisms involve disruption of the functional integrity of the bacterial membrane in a Ca-dependent manner. In the present work, we investigated the molecular basis of DAP resistance in a group of isogenic MRSA clinical strains obtained from patients with *S. aureus* infections after treatment with DAP. Different point mutations were found in the *mprF* gene in DAP-resistant (DR) strains. Investigation of the *mprF* L826F mutation in DR strains was accomplished by inactivation and transcomplementation of either full-length wild-type or mutated *mprF* in DAP-susceptible (DS) strains, revealing that they were mechanistically linked to the DR phenotype. However, our data suggested that *mprF* was not the only factor determining the resistance to DAP. Differential gene expression analysis showed upregulation of the two-component regulatory system *vraSR*. Inactivation of *vraSR* resulted in increased DAP susceptibility, while complementation of *vraSR* mutant strains restored DAP resistance to levels comparable to those observed in the corresponding DR wild-type strain. Electron microscopy analysis showed a thicker cell wall in DR CB5012 than DS CB5011, an effect that was related to the impact of *vraSR* and *mprF* mutations in the cell wall. Moreover, overexpression of *vraSR* in DS strains resulted in both increased resistance to DAP and decreased resistance to oxacillin, similar to the phenotype observed in DR strains. These results support the suggestion that, in addition to mutations in *mprF*, *vraSR* contributes to DAP resistance in the present group of clinical strains.

Staphylococcus aureus is the most common Gram-positive pathogen among skin and soft tissue infections (2). Methicillin resistance in *S. aureus* is mediated by the acquisition of a penicillin-binding protein (PBP), PBP 2a, which has decreased affinity for β-lactam antibiotics but can continue to cross-link the cell wall once the native PBPs (i.e., PBPs 1 to 4) have been inactivated (23). A distinctive feature for most methicillin-resistant *S. aureus* (MRSA) strains is the heterogeneous expression of resistance, characterized by a small proportion ($\leq$0.1%) of the population expressing a high level of homogeneous resistance while most of the other isolates in the population express resistance to 10 μg/ml (12, 15, 43). Daptomycin (DAP) is a cyclic anionic lipopeptide antibiotic that is produced by *Streptomyces roseosporus* (3) and is approved for treatment of skin and skin structure infections as well as treatment of bacteremia and right-side endocarditis caused by MRSA (1). The mechanism of action involves disruption of cytoplasmic membrane function, resulting in depolarization and cell death due to disruption of critical metabolic functions, such as protein, DNA, and RNA synthesis (2).

The incidence of DAP resistance in clinical isolates is very low, and resistant strains display small increases in MIC (2). The exact mechanism of DAP resistance has not yet been fully elucidated, although some characteristics of the resistance phenotype have been described. Genes regulating cell membrane surface charge (e.g., *mprF*, lysylphosphatidylglycerol [LPG] synthetase) and fatty acid biosynthesis (e.g., *yycFG*, two-component sensor kinase system) were associated with resistance (34, 40) in both laboratory-derived and clinical *S. aureus* strains (17). Other studies showed that at least four phenotypic membrane alterations correlated with DAP resistance in *S. aureus*, notably, in regard to the three major membrane components, phosphatidylglycerol, cardiolipin, and LPG (25). These studies demonstrated that DAP-nonsusceptible isolates exhibited enhanced outer leaflet LPG translocation compared to the daptomycin-susceptible isolates (25). The synthesis and the outer leaflet translocation of LPG are mediated by MprF (40), and a correlation between increased expression of a mutant *mprF* gene and reduced *in vitro* DAP susceptibility was recently reported (48). Moreover, it has been demonstrated that the *dltABCD* operon also contributes to the net membrane positive charge by *d*-alanylating wall teichoic acids (WTAs) through distinct effector mechanisms (5). Thus, the associated effect of both the *mprF* and *dltABCD* mechanisms would result in a reduced access of calcium-DAP to its membrane target. Besides the membrane, changes in the cell wall are suggested to be involved in DAP resistance. Recently, studies by Muthaiyan et al. demonstrated with transcriptional profiling that DAP is an inducer of the cell wall stress stimulon, affecting the expression of both genes that are involved in the peptidoglycan synthesis of *S. aureus* and those that are known to be under regulation of the

Received 31 March 2010 Returned for modification 12 July 2010
Accepted 27 September 2011
Published ahead of print 10 October 2011
Address correspondence to Adriana E. Rosato, aerosato@tmhs.org.

doi:10.1128/AAC.00432-10

VraSR two-component regulatory system (35). In this context, it has been observed in an *in vitro*-generated, DAP-nonsusceptible derivative strain that *vraSR* was upregulated, while expression of *mprF* was repressed; no mutations in *mprF* were observed in this strain (7).

The present work aimed to investigate the molecular basis of DAP resistance in pairs of DAP-susceptible (DS) and DAP-resistant (DR) isogenic MRSA clinical strains obtained as a result of DAP treatment failure. We found that both *mprF* point mutations and differential expression levels of *vraSR* observed between DS and DR strains were mechanistically linked to the DAP-resistant phenotype. Moreover, we observed that decreased susceptibility to DAP was associated in the majority of strains with increased susceptibility to oxacillin, a phenotype associated with their heterotypic mode of β-lactam resistance expression, i.e., in heterogeneous but not homogeneous MRSA strains. These results support the concept that increased expression of *vraSR* represents an additional factor contributing to the development of daptomycin resistance in these clinical MRSA strains.

MATERIALS AND METHODS

Materials and media. Trypticase soy agar (TSA II) with 5% sheep blood (BBL, Sparks, MD) and Mueller-Hinton agar (MHA; BBL Microbiology Systems, Cockeysville, MD) with and without additives (Sigma, St. Louis, MO; United States Biochemicals, Cleveland, OH) were used for subculture and maintenance of *S. aureus* strains.

Bacterial strains. All of the strains and primers used in this study are listed in Tables 1 and 2. Pulsed-field gel electrophoresis (PFGE) was used to determine the clonality of the isogenic strains as previously described (4, 45).

Antibiotics. Standard reference powders were obtained from Sigma-Aldrich, St. Louis, MO (oxacillin and vancomycin); DAP was provided by Cubist Pharmaceuticals, Lexington, MA. Susceptibilities to oxacillin and vancomycin were determined according to the guidelines of the Clinical and Laboratory Standards Institute (CLSI; formerly NCCLS) (36). Daptomycin MICs were determined by Etest (AB Biodisk, Solna, Sweden).

Population analysis. Population analysis profiles were determined as described by Chambers et al. (10). In the case of DAP population analysis, profiles were performed by using MHA supplemented with calcium (50 μg/ml) and containing increasing concentrations of DAP, and 10^9 CFU from an overnight culture was serially diluted as the inoculum.

Comparison of relative net cell surface charge. Previous investigations indicated that DR *S. aureus* strains are associated with frequent alteration of the net cell surface charge compared to that of the respective DS parental strains (25, 32). For these assays, we compared the relative net cell surface charge of pairs CB5011/CB5012, CB5035/CB5036, and CB182/CB183 by quantifying the association of the highly cationic molecule cytochrome *c* (pI 10; Sigma) to the staphylococcal surface. The amount of cytochrome *c* remaining in the postcentrifugation supernatant after a 10-min binding interaction with *S. aureus* cells was quantified spectrophotometrically at an optical density at 530 nm (OD_{530}). The more unbound cytochrome *c* that was detected in the supernatant, the more that a positive charge existed on the bacterial cell surface. Strains CB685 and CB687 were used as controls (*dltA* positive and negative), respectively (41). The data shown are the means ($\pm$ standard deviations [SDs]) of the amount of unbound cytochrome *c* from three independent experiments.

Determination of SCC*mec* types. Chromosomal DNA was prepared by using a Qiagen (Valencia, CA) genomic DNA preparation kit according to the manufacturer's instructions. Staphylococcal cassette chromosome *mec* (SCC*mec*) types were determined as previously described (38). *S. aureus* strains COL (SCC*mec* type I), N315 (SCC*mec* type II), ANS46 (SCC*mec* type III), and USA300 (SCC*mec* type IV) were used as positive controls.

Analysis of gene expression by real-time RT-PCR, Northern blotting, and microarray transcriptional profiling. RNA extractions for real-time reverse transcription-PCR (RT-PCR) and Northern blot analyses were performed as previously described (12, 19, 44). Total RNA was extracted using an RNeasy isolation kit (Qiagen); all RNA samples were analyzed by A_{260}/A_{280} spectrophotometry and gel electrophoresis to assess concentration and integrity and cleaned of potential DNA contamination by treating them with DNase as per manufacturer recommendations (Ambion, Inc., Austin, TX). Real-time reverse transcription-PCR analysis was done using a SensiMix SYBR One-Step kit (Quantace/Bioline, Taunton, MA) according to the manufacturer's protocol. Gene expression was compared according to the threshold cycle (C_T) values converted to fold change with respect of a sample considered the reference (value = 1) using $\log_2 -(\Delta\Delta C_T)$. The change (*n*-fold) in the transcript level was calculated using the following equations: $\Delta C_T = C_{T(\text{test DNA})} - C_{T(\text{reference cDNA})}$, $\Delta\Delta C_T = \Delta C_{T(\text{target gene})} - \Delta C_{T(\text{16S rRNA})}$, and ratio $= 2^{-\Delta\Delta CT}$ (30). The quantity of cDNA for each experimental gene was normalized to the quantity of 16S cDNA in each sample determined in a separate reaction. Each RNA sample was run in triplicate; values represent the means of at least three separate RNA samples. Oligonucleotide primers are shown in Table 2.

Northern blot analysis was performed by using 7 μg of RNA separated through formaldehyde-containing 1% agarose. The intensities of the 23S and 16S rRNAs were visualized using a 254-nm UV shortwave lamp, and quantities were adjusted so that the same amount of RNA was loaded for each sample. RNA was transferred from agarose to positively charged nylon membranes (Stratagene, La Jolla, CA) by capillary action (44). Labeling and hybridization were done using digoxigenin labeling and detection kits (Roche, Indianapolis, IN) according to the manufacturer's instructions. Oligonucleotide primers are shown in Table 2.

Microarray transcriptional profiling was carried out as previously described (12, 19) by using a spotted DNA microarray (J. Craig Venter Institute, version 6 *S. aureus* slides) containing 4,546 oligonucleotides (70-mer) covering the genomes of *S. aureus* COL (2,654 open reading frames [ORFs]), *S. aureus* N315 (2,623 ORFs), *S. aureus* Mu50 (2,748 ORFs), MRSA 252 (2,744 ORFs), MSSA 476 (2,619 ORFs), and pLW043 (62 ORFs). Pairwise comparisons, performed in triplicate, between isogenic pairs A (CB5011 versus CB5012), E (CB5035 versus CB5036), and F (CB182 versus CB183) were made, as indicated in Table 1.

The comparisons were performed between DS and DR MRSA isogenic pairs grown in drug-free LB medium collected at exponential growth (log) phase (OD_{600}, 0.6). The results are based on a series of statistical analyses (filtering) where ratios of Cy3 and Cy5 were converted to $\log_2$ values and the cutoff was set at above 1 (present) or below -1 (absent) (8, 12). Median signal intensity values, calculated from each set of in-slide replicates and flipped-dye experiments, were used to calculate $\log_2$ and *n*-fold changes in gene expression. The data set was normalized by applying the LOWESS algorithm (block mode; smooth parameter, 0.33) and using MIDAS software (http://www.jcvi.org/cms/research/software/), and significant changes were identified with SAM (significance analysis of microarrays) software (http://www-stat.stanford.edu/tibs/SAM/index.html) (8, 12).

Cloning, transformation, and DNA manipulation. All restriction endonuclease digestions and ligations were performed in accordance with the manufacturer's (New England BioLabs, Beverly, MA) specifications. Chromosomal DNA was prepared by using a Qiagen genomic DNA preparation kit according to the manufacturer's directions. Sequencing of all PCR amplification products was performed by the Nucleic Acid Research Facility at Virginia Commonwealth University (Richmond, VA). Sequence analysis of *mprF* from clinical isolates was performed using chromosomal DNA isolated from DS/DR strains at SeqWright (Houston, TX); primers used were previously described (17, 26, 42). Consensus sequences were assembled from both orientations with Vector NTI Advance 10 software for Windows (InforMax, Bethesda, MD). *S. aureus* N315 (GenBank accession number BA000018) was used as a positive control.

TABLE 1 Description of strains and plasmids used in this study

Strain[a]	Relevant genotype and phenotype	Reference or source
S. aureus		
COL	Methicillin-resistant SCC*mec* type I	10
N315	Methicillin-resistant SCC*mec* type II	29
USA300	Methicillin-resistant SCC*mec* type IV	9, 27
CK1001	RN4220 Δ*mprF*::*cat*	22
KVR	N315Δ*vraSR*::*cat*	28
RN4220	Restriction-deficient mutagenized RN450	15
CB5011, pair A	DS, SCC*mec* type II (USA100)	Cubist Pharmaceuticals
CB5012, pair A	DR isogenic to CB5011; MprF L826F	Cubist Pharmaceuticals
CB5013, pair B	DS, SCC*mec* type II (USA100)	Cubist Pharmaceuticals
CB5014, pair B	DR isogenic to CB5013, MprF S377L	Cubist Pharmaceuticals
CB1631, pair C	DS, SCC*mec* type II (USA100)	Cubist Pharmaceuticals
CB1634, pair C	DR isogenic to CB1631, MprF L826F	Cubist Pharmaceuticals
CB5048, pair D	DS, SCC*mec* type IV (USA300)	Cubist Pharmaceuticals
CB5051, pair D	DR isogenic to CB5048	Cubist Pharmaceuticals
CB5035, pair E	DS, SCC*mec* type II (USA100)	Cubist Pharmaceuticals
CB5036, pair E	DR isogenic to CB5035, MprF P314L	Cubist Pharmaceuticals
CB182, pair F	DS, SCC*mec* type IV (USA300)	Cubist Pharmaceuticals
CB183, pair F	DR isogenic to CB182, MprF L341S	Cubist Pharmaceuticals
Derivative *S. aureus* strains		
MAR-1	CB5011 Δ*mprF*::*cat*	This study
MAR-2	MAR-1 + pMPRF-1 (wild-type *mprF* cloned into pPV72-2)	This study
MAR-3	MAR-1 + pMPRF-2 (mutated *mprF* L826F cloned into pPV72-2)	This study
MAR-4	CB5012+ Δ*mprF*::*cat*	This study
MAR-5	MAR-4 + pMPRF-1	This study
MAR-6	MAR-4 + pMPRF-2	This study
MAR-7	CB5012 Δ*vraSR*::*cat*	This study
MAR-8	MAR-7 + pVRASR-2	This study
MAR-9	CB5011 expressing pVRASR-2	This study
MAR-10	CB5013 expressing pVRASR-2	This study
MAR-11	CB1631 expressing pVRASR-2	This study
MAR-12	CB5048 expressing pVRASR-2	This study
MAR-13	CB5035 expressing pVRASR-2	This study
MAR-14	CB1631 Δ*mprF*::*cat*	This study
MAR-15	MAR-14 pMPRF-1 (wild-type *mprF* cloned into pPV72-2)	This study
MAR-16	MAR-14 pMRPF-2 (mutated *mprF* L826F cloned into pPV72-2)	This study
MAR-17	CB1634 Δ*mprF*::*cat*	This study
MAR-18	MAR-17(pMPRF-1) (wild-type *mprF* cloned into pPV72-2)	This study
MAR-19	MAR-17(pMRPF-3) (mutated *mprF* L826F cloned into pPV72-2)	This study
E. coli (PCR2.1-TOPO)	Amp^r Kan^r	Invitrogen
S. aureus (pPV72-2)	Shuttle vector; *E. coli*-*S. aureus* Tet^r	31
S. aureus RN4220 (pVRASR-2)	Entire *vraS*/*vraR* cloned into pAW8	6
S. aureus RN4220 (pMPRF-1)	Entire *mprF* cloned into pPV72-2	This study
S. aureus RN4220 (pMPRF-2)	Full-length *mprF* containing L826F site-directed mutation from CB5012 cloned into pPV72-2	This study
S. aureus RN4220 (pMPRF-3)	Full-length *mprF* containing L826F site-directed mutation from CB1634 cloned into pPV72-2	This study

[a] Pair A, parent strain CB5011 and its derivative, CB5012; pair B, CB5013 and derivative CB5014; pair C, CB1631 and derivative CB1634; pair D, CB5048 and derivative CB5051; pair E, CB5035 and derivative CB5036; pair F, CB182 and derivative CB183.

Mutational insertion inactivation of *mprF* and complementation. *mprF*-null mutants were constructed by moving Δ*mprF*::*cat* from strain CK1001 (22) into the clinical DR MRSA strains CB5012 and CB1634 and their DS counterparts, CB5011 and CB1631, respectively, by general transduction using 80α phage (37). Transcomplementation of *mprF* was performed by using a construct encompassing the complete *mprF* gene as well as the upstream region (425 bp) including the putative ribosomal binding site and promoter using *mprF* primers *mprF*-F2 and *mprF*-R2, shown in Table 2. The 3.0-kb PCR fragment products were purified using a QIAquick gel extraction kit, ligated into the ligase-independent cloning site of the PCR2.1-TOPO vector (Invitrogen, Carlsbad, CA), and transformed into chemically competent *Escherichia coli* TOP10 cells (Invitrogen). A staphylococcal origin of replication was introduced by cloning

TABLE 2 Primers used in this study[a]

Primers	5′–3′
16S-F	TCCGGAATTATTGGGCGTAA
16S-R	CCACTTTCCTCTTCTGCACTCA
vraSR-R	GGTGCAACGTTCCATATTGTATTGT
vraSR-F	GGCTTCAACTCATGGGCTTTGGCAA
mecA-F	TGCCTAATCTCATATGTGTTCCTGTAT
mecA-R	CGGTGCTGAAACTTATTCACAATATAAT
mprF-F	GTGGCGACATTCTTCACTTACG
mprF-R	GCCAGAAGTAATAGCGCAATACAG
mprF-F2	ATGTTGGGCAGTTACATTTATGAT
mprF-R2	GACTTAACTTAAGCTCATTTC

[a] All primers were prepared for this study.

plasmid pPV72-2, an *S. aureus* replicon (31), into the unique BamHI site on PCR 2.1-TOPO (pMPRF-1; Table 1); the construct was moved into *S. aureus* RN4220 by electroporation (15). Transcomplementation of *mprF* mutants was obtained by transduction of plasmid pMPRF-1 (pPV72-2 vector containing wild-type *mprF*) from RN4220 by phage 80α into DR *mprF* mutants CB5012 Δ*mprF*::*cat* and CB1634 Δ*mprF*::*cat* and into their counterpart DS *mprF* mutants, CB5011 Δ*mprF*::*cat* and CB1631Δ*mprF*::*cat*, respectively. In addition, CB5012 Δ*mprF*::*cat* and CB5011 Δ*mprF*::*cat* mutants were transduced with pMPRF-2 (pPV72-2 harboring full-length *mprF* containing an L826F site-directed mutation), obtaining MAR-3 (CB5011Δ*mprF*::*cat*) and MAR-6 (CB5012 Δ*mprF*::*cat*), respectively. This was similarly performed for mutants CB1631Δ*mprF*::*cat* and CB1634 Δ*mprF*::*cat* by introducing pMPRF-3 (pPV72-2 harboring full-length *mprF* containing L826F), obtaining MAR-16 and MAR-19, respectively. All constructs were verified by both sequence and restriction enzyme analyses.

Construction of *vraSR*-null mutants and complementation. A mutant MAR-7 strain (Table 1) was obtained by transducing the deletion *vraSR* mutant (Δ*vraSR*::*cat*) by ϕ11 phage from strain KVR (28) into DR CB5012 (37). The mutant MAR-7 was transcomplemented with a shuttle plasmid, pAW8, containing a 3.3-kb fragment corresponding to the entire *vraSR* operon (6) by transduction, resulting in the MAR-8 strain (Table 1). Overexpression of *vraSR* in DS strains CB5011, CB5013, CB1631, CB5048, and CB5035 was performed by phage 80α-mediated transduction of shuttle plasmid pAW8 containing the entire *vraSR* operon (6), resulting in strains MAR-9 to MAR-13, respectively (Table 1).

Electron microscopy (EM) evaluation of cell wall thickness. The preparation of *S. aureus* cells for transmission electron microscopy from DS parent CB5011, DR derivative CB5012, and genetically modified mutant derivative strains was performed using standard procedures described by Cui et al. (11). Briefly, morphometric evaluation of cell wall thickness was performed by using photographic images at a final magnification of ×30,000. Thirty cells of each strain with nearly equatorial cut surfaces were measured for the evaluation of cell wall thickness, and results were expressed as means ± SDs. All of the cell wall thickness measurements were performed by two of the listed authors (S.M. and K.B.P.), who were blinded to the identities of the organisms.

RESULTS

Phenotypic studies between DS and DR MRSA pairs. DAP, oxacillin, and vancomycin MICs were determined in six isogenic DS/DR strains labeled pairs A, B, C, D, E, and F by using standard procedures, including the Etest (AB Biodisk, Dalvagen, Sweden) in medium supplemented with calcium (50 μg/ml $CaCl_2$). We found an increase in DAP MICs in all DR strains (2 to 4 μg/ml) that was associated with a slight decrease in vancomycin susceptibility (1 to 3 μg/ml); baseline daptomycin and vancomycin MICs were 0.25 to 0.5 μg/ml and 1 to 2 μg/ml for the DS and DR strains, respectively (Table 3). No changes in susceptibility to cationic molecules such as gentamicin were observed between DS-DR strains (data not shown). We next investigated the expression of resistance to DAP by population analysis profile. As shown in Fig. 1A, for pair A, 5×10^5 DS CB5011 cells were inhibited at 0.5 μg/ml, while 3×10^8 DR CB5012 cells were still growing at the same DAP concentration. Similar results were obtained for pairs D and E (data not shown). Interestingly, susceptibility to oxacillin was reduced from 16 to 32 μg/ml to 1 to 0.25 μg/ml in DR strains for pairs A, C, D, and F; pairs B and E did not show changes in oxacillin MICs (512 μg/ml) (Table 3). Analysis of oxacillin resistance expression showed a typical heterogeneous MRSA profile in pairs A, C, D, and F, in which, for example, 9×10^3 DS CB5011 cells grew at an oxacillin concentration of 32 μg/ml, while its DR CB5012 counterpart (4×10^3 cells) was inhibited at an oxacillin concentration of 0.25 μg/ml (Fig. 1B). In contrast, pairs B and E displayed a homogeneous oxacillin expression profile with no reduction in oxacillin susceptibility (Fig. 1C). These results suggest that in this group of strains, DAP resistance is associated with a concomitant decrease in oxacillin resistance in MRSA strains expressing heterogeneous β-lactam resistance.

TABLE 3 MICs of *S. aureus* DS and DR strains against DAP, oxacillin, and vancomycin

Pair	Strain (DAP susceptibility)	MIC (μg/ml)[a]		
		DAP	OXA	VAN
A	CB5011 (DS)	0.5	32	1
	CB5012 (DR)	4	0.25	2
B	CB5013 (DS)	0.5	512	1
	CB5014 (DR)	4	512	2
C	CB1631 (DS)	0.5	32	1
	CB1634 (DR)	4	0.5	2
D	CB5048 (DS)	0.25	32	1.5
	CB5051 (DR)	2	1	2
E	CB5035 (DS)	0.25	512	1.5
	CB5036 (DR)	2	512	3
F	CB182 (DS)	0.5	32	1
	CB183 (DR)	4	1	2

[a] OXA, oxacillin; VAN, vancomycin.

Previous studies have shown that DR *S. aureus* strains displayed a frequent alteration of the net cell surface charge compared to their DS counterparts (14). By spectrophotometrically quantifying the amount of bound cytochrome *c*, we found no significant changes between DS/DR strain pairs CB5011/CB5012, CB5035/CB5036, and CB182/CB183 (Table 1; Fig. 2). The pair CB685 and CB687 (*dltA* positive and negative, respectively) was used as a positive control. As previously reported (41), strain CB687displayed increased levels of bound cytochrome *c* compared to strain CB685 (Fig. 2). The resistant isolates tested herein (Fig. 2) were not significantly different from their parent, susceptible isolates, suggesting that these data are consistent with, although do not completely exclude, the possibility that changes in cell surface charge are not a significant contributor to the mechanism associated with the resistance phenotype in the present group of clinical strains.

Genotypic analysis of DS/DR MRSA strains. To determine whether DAP resistance was linked to a specific SCC*mec* structure, we performed a multiplex PCR analysis of the *ccrAB* genes, implicated in the excision and integration of SCC*mec* to the *S. aureus* chromosome (38). We determined that pairs A, B, C, and E display an SCC*mec* type II structure characterized by the presence of *mecA*, the regulators *mecI*/*mecR1*, and the *ccrAB2* genes, a profile that was identical to that for the positive-control *S. aureus* N315 (SCC*mec* type II element) strain and related to that of USA100-type strains. In contrast, pairs D and F harbored SCC*mec* type IV and were related to USA300-type strains, with the insertion of the IS*1272* element at the 3′-terminal portion of the regulator *mecR1* and deletion of the repressor *mecI* (data not shown). In addition, PFGE analysis performed with DS/DR pair strains indicated clonality with an absence of genomic rearrangements (data not shown). Together, these results led us to infer that the decrease in oxacillin resistance observed in the above-mentioned DR strains was not due to deletion of SCC*mec* and/or *mecA* (data not shown).

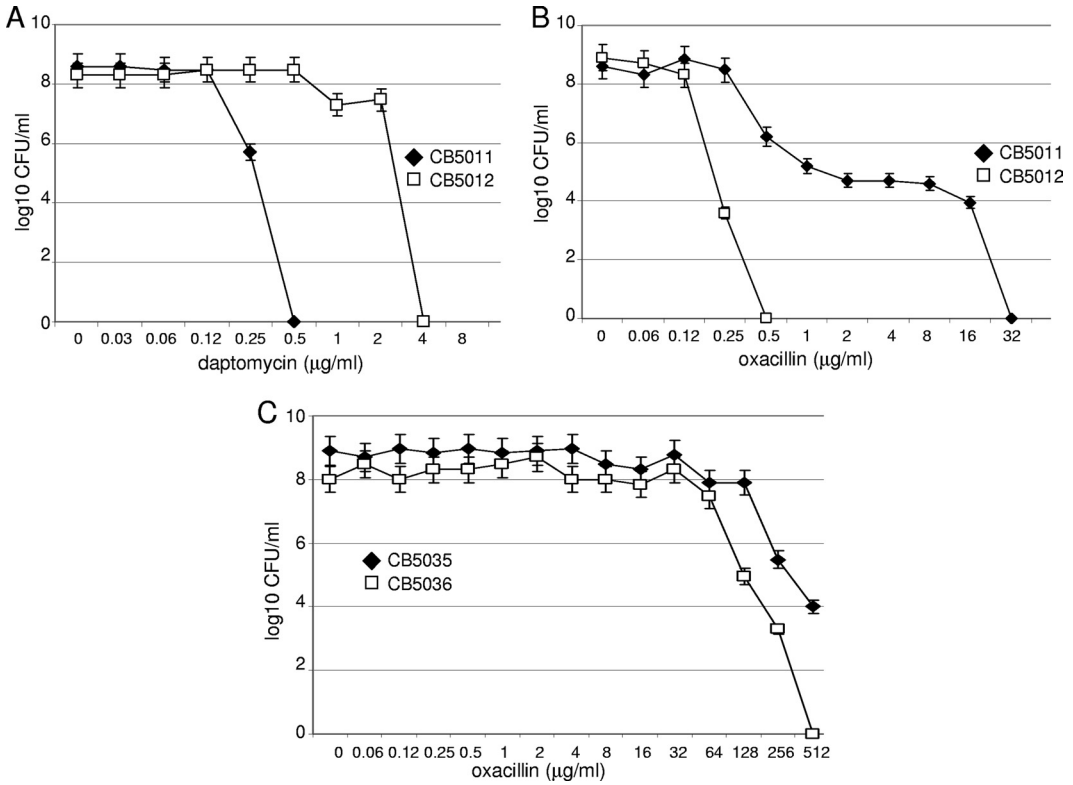

FIG 1 Population analysis profiles. Aliquots (10 μl) from overnight LB cultures of the DS CB5011 and DR CB5012 (A and B) and DS CB5035 and DR CB5036 (C) *S. aureus* strains were inoculated to MHA plates containing increasing concentrations of daptomycin (with Ca^{2+} at 50 mg/liter) (A and B) and oxacillin (C) to determine the mode of phenotypic expression of resistance by population analysis, as described in Materials and Methods.

Mutations in the *mprF* gene contribute to DAP resistance in DS/DR MRSA pairs. Previous studies have shown that resistance to DAP in either clinical MRSA or laboratory mutant strains may be associated with changes in *mprF*, including increased transcription and/or point mutations leading to a gain-of-function phenotype (40, 48). To determine whether similar events may account for resistance to DAP in our clinical MRSA strains, we performed expression analysis of *mprF* by real-time RT-PCR using RNA extracted from DS and DR cells collected at both exponential and stationary phases of growth (OD_{600}s, 0.6 and 1.0, respectively). No significant difference between DS and DR strains was observed (data not shown), suggesting that DAP resistance in our clinical DR MRSA strains is not mediated through increased *mprF* expression. Sequence analysis of *mprF* revealed the presence of the following mutations: pair A, DR CB5012, one amino acid substitution, leucine 826 to phenylalanine (L826F); pair B, DR CB5013, S377L; pair C, DR CB1631, L826F; pair E, DR CB5036, P314L; and pair F, DR CB183, L341S (Table 1). Three single amino acid sub-

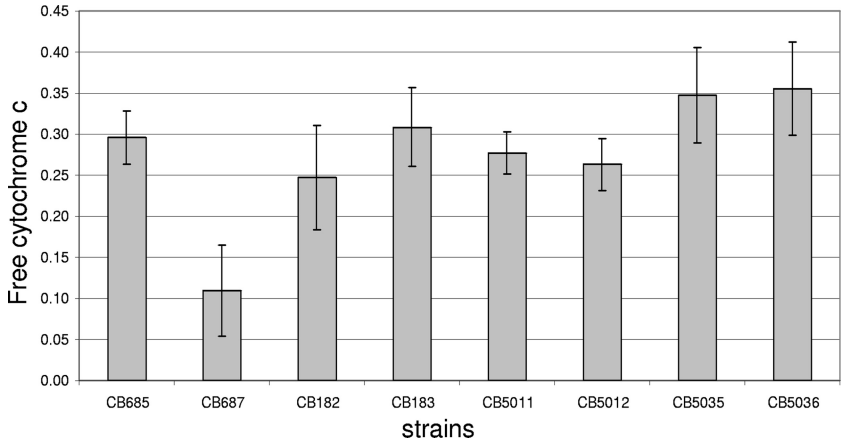

FIG 2 Binding of positively charged cytochrome *c* to whole DS-DR MRSA cells. The graph shows the percentage of cytochrome *c* unbound after 10 min incubation with the DS-DR cells at room temperature. Strains CB685 and CB687 (*dltA* positive and negative, respectively) were used as positive controls. Data represent the means and standard deviations from three independent experiments.

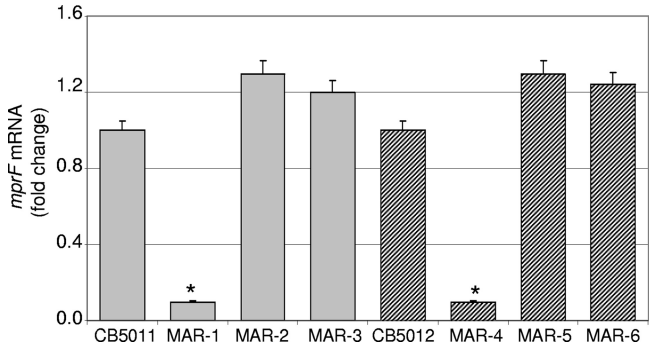

FIG 3 Quantitation of *mprF* mRNA by real-time RT-PCR. RNA was prepared from cells of DS CB5011, *mprF*-null mutant MAR-1, MAR-1 *mprF*-complemented MAR-2 and MAR-3, DR CB5012, *mprF*-null mutant MAR-4, and MAR-4 *mprF*-complemented MAR-5 and MAR-6 strains collected at exponential phase of growth, as described in Materials and Methods. Relative fold change values of specific *mprF* mRNA are shown on the vertical axis; 16S rRNA was used as an internal control. *, significantly less than control ($P < 0.001$).

stitutions were mapped to the hydrophobic N-terminal translocase domain of MprF (i.e., S377L, P314L, and L341S), while the substitution L826F localized to the hydrophilic Lys1-phosphatidylglycerol synthase C-terminal portion (14). To determine the potential role of *mprF* mutations in DAP resistance, an *mprF* null mutant was generated, using as background the DS CB5011 strain, by 80α-mediated transduction from *mprF*-null mutant strain CK1001 (22). The resulting strain (MAR-1; Table 1) was verified by both PCR (DNA) and real-time RT-PCR (RNA) (Fig. 3). Mutant MAR-1 (CB5011 Δ*mprF*::*cat*) was complemented either with pMPRF-1 containing the wild-type full-length *mprF* gene cloned in pPV72-2 (CB5011 Δ*mprF*::*cat* plus pMPRF-1, strain MAR-2; Table 1) or with pMPRF-2 harboring the full-length *mprF* gene containing the L826F site-directed mutation (CB5011Δ*mprF*::*cat* plus pMPRF-2, strain MAR-3; Table 1). *mprF* expression was verified following complementation in RNA samples prepared from cells collected at the exponential phase of growth (OD_{600}, 0.6); *mprF* transcomplementation (strains MAR-2 and MAR-3; Table 1) resulted in *mprF* transcription levels similar to those observed in parental strain CB5011 (Fig. 3). Similar results of *mprF* expression were obtained in *mprF* mutants (MAR-14 and MAR-19; data not shown). Phenotypic analysis was then performed between the *mprF* mutant (MAR-1) and complemented MAR-2 and MAR-3 strains. MIC values showed a decrease in DAP MIC in MAR-1 compared to wild-type CB5011 (MICs, 0.094 μg/ml and 0.5 μg/ml, respectively; Table 4). Complementation of the MAR-1 strain with wild-type *mprF* (MAR-2) restored the DAP MIC to a level equivalent to that of CB5011 (0.5 μg/ml); however, full-length *mprF* containing the L826F mutation resulted in an increased DAP MIC, up to 2 μg/ml (MAR-3; Table 4), despite levels of transcription similar to those existing in the wild-type strain (Fig. 3).

Inactivation of *mprF* was then performed in the DR CB5012 strain by transduction with phage lysates from *mprF*-null mutant CK1001 (22), and lack of expression of *mprF* was verified by real-time RT-PCR (MAR-4; Fig. 3). Phenotypic analysis of MAR-4 revealed that inactivation of *mprF* increased susceptibility to DAP (MICs, 4 μg/ml and 0.5 μg/ml for CB5012 and MAR-4, respectively; Table 4). As with the DS CB5011 strain, complementation of the *mprF* mutant MAR-4 strain with wild-type full-length *mprF* (MAR-5) resulted in a DAP MIC of 0.75 μg/ml (Table 4), while complementation of MAR-4 with *mprF* L826F conferred higher resistance to DAP (MAR-6; MIC, 3 μg/ml; Table 4). To further investigate whether the L826F *mprF* mutation was responsible for the observed phenotype and was not due to a secondary effect related to the plasmid expression, a similar approach was performed in the pair CB1631 (DS) and CB1634 (DR) containing the same L826F *mprF* mutation. Results shown in Table 4 confirmed the observations established in pair CB5011/CB5012. Together, in agreement with previous observations (17, 26, 42), these results indicate that mutations observed in *mprF* may contribute to decreased susceptibility to DAP in DR strains. However, they also suggest that the introduction of only these mutations may not be sufficient to achieve the level of resistance observed in DR strains, as suggested by studies performed using the DS strain background. Further studies designed to establish the functional significance of *mprF* mutations detected in other pairs are ongoing.

Analysis of differentially expressed genes by spotted microarrays in isogenic DS/DR MRSA clinical strains. We performed differential gene expression analysis by spotted DNA microarray to identify additional mechanisms that may be involved in establishing resistance to DAP. This analysis was determined in three of the pairs used in the present investigation, i.e., pair A (CB5011 [DS] versus CB5012 [DR]), pair E (CB5035 [DS] versus CB5036 [DR]), and pair F (CB182 [DS] versus CB183 [DR]) (Table 5). As shown in Table 5, overall changes in expression levels of most genes were moderate, with ratios in the range of 2- to 5-fold. On the basis of a cutoff value arbitrarily set at a 2-fold change, genes upregulated in DR versus DS strains in the above-mentioned pairs included genes related to cell wall metabolism, *mecA* (SA0038_N315) and penicillin-binding protein 2, *pbp2* (SA1283_N315); two-component sensor histidine kinase *vraS* (SA1701_N315) and two-component response regulator *vraR* (SA1700_N315), which play a major role in sensing and reacting to cell wall stress; and the peptidoglycan synthesis (elongation) gene *sgtB* (SA1691_N315). Other upregulated genes were *vraF* (ABC transporter ATP-binding protein, SA0616_N315) and *vraG* (ABC transporter permease, SA0617_N315), known to be in-

TABLE 4 Daptomycin MICs of *mprF*-null mutant and *mprF*-complemented strains

Strain	Genotype	MIC (μg/ml)
CB5011	DS	0.5
MAR-1	CB5011 Δ*mprF*::*cat*	0.094
MAR-2	MAR-1 + pMPRF-1	0.5
MAR-3	MAR-1 + pMPRF-2	2
CB5012	DR	4
MAR-4	CB5012 + Δ*mprF*::*cat*	0.5
MAR-5	MAR-4 + pMPRF-1	0.75
MAR-6	MAR-4 + pMPRF-2	3
CB1631	DS	0.25
MAR-14	CB1631 Δ*mprF*::*cat*	0.064
MAR-15	MAR-14 + pMPRF-1	0.5
MAR-16	MAR-14 + pMPRF-3	2
CB1634	DR	4
MAR-17	CB1634 Δ*mprF*::*cat*	0.5
MAR-18	MAR-17 + pMPRF-1	0.5
MAR-18	MAR-17 + pMPRF-3	3

TABLE 5 Differential gene expression between DS and DR strains[a]

ORF	Gene	Product or putative function	Fold change
SA0616_N315	*vraF*	ABC transporter ATP-binding protein	+3.8
SA0617_N315	*vraG*	ABC transporter permease	+4.3
SA2312_N315	*ddh*	2-Hydroxyacid dehydrogenase	+3.1
SA2254_N315	*opp-1B*	Oligopeptide transporter putative membrane permease domain	+3.5
SA1211_N315	*opp-2F*	Oligopeptide transporter putative ATPase domain	+3.5
SA0038_N315	*mecA*	PBP 2a	+4.2
SA1283_N315	*pbp2*	PBP 2	+4.5
SA1691_N315	*sgtB*	Elongation of peptidoglycan synthesis	+3.2
SA1023_N315	*ftsL*	Cell division protein	+4.4
SA1700_N315	*vraR*	Two-component response regulator	+5.5
SA1701_N315	*vraS*	Two-component sensor histidine kinase	+4.7
SA0661_N315	*saeR*	Response regulator	+3.1
SA0760_N315		Glycine cleavage system protein H	+4.1
SA1458_N315	*lytH*	*N*-Acetylmuramoyl-L-alanine amidase	+3.8
SA0149_N315	*capF*	Capsular polysaccharide synthesis enzyme Cap5F	+2.8
SACOL2509	*fnbB*	Fibronectin binding protein	−3.3
SA0747_N315	*cspC*	Cold shock protein	−4.3
SAR2790	*cspB*	Cold shock protein	−3.8
SA1141_N315	*glpK*	Glycerol kinase	−3.5
SA1140_N315	*glpF*	Glycerol uptake facilitator	−4.6
SA1126_N315	*pgsA*	Phosphatidylglycerophosphate synthase	−2.6
SA1272_N315		Alanine dehydrogenase	−4.5
SA1365-N315		Glycine dehydrogenase subunit 2	−3.2
SA1047-N315	*pryF*	Orotidine-5-phospate decarboxylase	−3.1
SA2425_N315	*arcC*	Carbamate kinase	−4.2
SA0253_N315	*lrgB*	Antiholin-like protein LrgB	−4.8
SA2499_N315	*gidB*	Glucose-inhibited division protein B	−2.7

[a] Analysis of strain pairs A (CB5011 [DS] versus CB5012 [DR]), E (CB5035 [DS] versus CB5036 [DR]), and F (CB182 [DS] versus CB183 [DR]); analysis of each pair was performed in triplicate. The data were normalized by applying the LOWESS algorithm (block mode; smooth parameter, 0.33) and using MIDAS software (http://www.jcvi.org/cms/research/software/), and significant changes were identified with SAM software. Values are averages of the three pairs analyzed.

volved in mechanisms of transport (7); *ddh* (2-hydroxyacid dehydrogenase, SA2312_N315); *opp-1B* (SA2254_N315, oligopeptide transporter putative membrane-permease domain); and *opp-2F* (SA1211_N315, oligopeptide transporter putative ATPase domain). Among downregulated genes, the analysis revealed *lrgB* (antiholin-like protein LrgB, SA0253_N315), a genetic locus reported to influence autolysis, with LrgB proteins acting as antiholins that regulate the activity of the holin CidA and CidB proteins, and a group involved in the metabolism of glycerol, including *glpF* (glycerol uptake facilitator, SA1140_N315), *pgsA* (phosphatidylglycerophosphate synthase, SA1126_N315), and dehydrogenases (alanine dehydrogenase, SA1272_N315; glycine dehydrogenase, SA1365_N315) (Table 5). These results indicate that genes involved in both cell wall and membrane synthesis may play a role during the acquisition of DAP resistance in the DR strains described herein.

Daptomycin resistance is functionally associated with increased expression of the *vraSR* regulon in clinical MRSA strains. Taking into account results from gene expression analysis described above (genes involved in cell wall synthesis and turnover) and previous studies showing that the two-component regulator and cell wall stress stimulon VraSR is involved in the action of DAP (7, 35) prompted us to characterize the role of *vraSR* in our strains. Changes in the expression of *vraSR* were further analyzed by RT-PCR and Northern blot analysis using RNA from DS and DR cells corresponding to pairs A through E. As shown in Fig. 4A, increased expression of *vraSR* was observed in all DR strains compared to their DS counterparts. To define the mechanistic significance of *vraSR* upregulation, the *vraSR* operon was inactivated in DR strains CB5012 (pair A, CB5012 Δ*vraSR*::*cat* [MAR-7]; Table 1) and CB5014 (pair B, CB5014 Δ*vraSR*::*cat*) by phage 11-mediated transduction from the *vraSR*-null mutant KVR (28). Lack of expression of *vraSR* in mutant strains was monitored by real-time RT-PCR. Phenotypic analysis of *vraSR*-null mutant MAR-7 by DAP Etest showed an increase in DAP susceptibility compared to the parental CB5012 strain (MICs, 0.25 μg/ml versus MIC 4 μg/ml); similar results were observed in *vraSR*-null mutant strain CB5014 Δ*vraSR*::*cat* (data not shown). *vraSR*-null mutant MAR-7 was then complemented with a cloned full-length *vraSR* (6) (MAR-8; Table 1). *vraSR* complementation was verified by RT-PCR and resulted in *vraSR* transcription levels similar to those corresponding to DR CB5012 (Fig. 4B); as expected, no changes in *vraSR* expression were observed in MAR-7 complemented with an empty vector (Fig. 3B). Phenotypic analysis of the MAR-8 strain showed that *vraSR* complementation restored DAP resistance with MICs of 0.25 μg/ml versus 3 μg/ml for MAR-7 and MAR-8, respectively, values comparable to those observed in CB5012 (pair A; Table 3).

To determine the mechanistic role of increased *vraSR* expression in daptomycin resistance, additional studies were performed by overexpressing *vraSR* in DS CB5011, CB5013, CB1631, CB5048, and CB5035 strains; complementation resulted in expression levels similar to those observed in the corresponding DR strains determined by RT-PCR (Fig. 4C). Phenotypic differences were determined by DAP MIC analysis; an increase in DAP MIC was consistently observed in *vraSR*-complemented DS strains, with values ranging from 2 μg/ml to 6 μg/ml (Table 6). Interest-

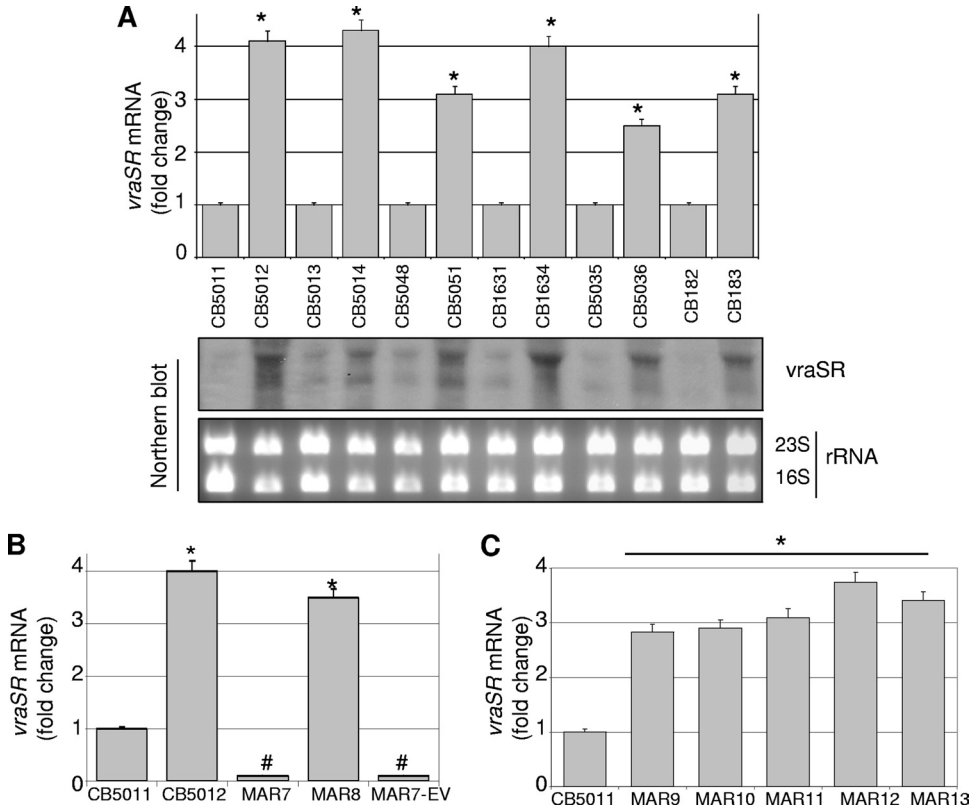

FIG 4 Quantitation of *vraSR* mRNA by real-time RT-PCR and Northern blot analysis. RNA was prepared from DS and DR cells (Table 1) grown in the absence of DAP and collected at exponential phase of growth, as described in Materials and Methods. (A, top) relative fold change values of specific *vraSR* mRNA are shown on the vertical axis; 16S rRNA was used as an internal control. *, significantly greater than control ($P < 0.001$). (A, bottom) Increase of VraSR transcription in DR strains compared to DS strains examined in the same group of strains for which fold change results are shown in the top panel. Ethidium bromide-stained 23S and 16S rRNA bands are shown below the Northern blots as loading controls. (B) Quantitation of *vraSR* mRNA by real-time RT-PCR in DS/DR CB5011/CB5012 strains (negative and positive *vraSR* controls, respectively), *vraSR*-null mutant MAR-7, and *vraSR*- or empty vector-complemented MAR-8 and MAR-7EV strains, respectively. RNA was prepared from cells grown and collected at exponential phase of growth. Relative values of specific *vraSR* mRNA are shown in the vertical axis; 16S rRNA was used as an internal control. *, significantly greater than control ($P < 0.001$); #, significantly less than DR CB5012 ($P < 0.01$). (C) Quantitation of *vraSR* mRNA by real-time RT-PCR in DS *vraSR*-overexpressing MAR-9 to MAR-13 strains. CB5011 (DS) was included as a control. Relative fold change values of specific *vraSR* mRNA are shown on the vertical axis; 16S rRNA was used as an internal control.*, significantly greater than sample CB5011 (DS) ($P < 0.001$). In all cases, three independent cultures were sampled in triplicate to minimize error caused by inter- and intrasample variation.

ingly, increases in DAP resistance after *vraSR* overexpression in DS strains were associated with a decrease in oxacillin resistance (e.g., oxacillin MICs, 0.5 μg/ml versus 32 μg/ml for MAR-9 and DS CB5011, respectively; Table 6), reflecting relationships between DAP and oxacillin phenotypes similar to those described in the original DS/DR strains (Table 3).

TABLE 6 MICs to DAP and oxacillin determined in DS and DS *vraSR*-overexpressing derivative strains

Strain	Genotype	MIC (μg/ml)	
		DAP	OXA[a]
MAR-9	CB5011 (DS)	0.5	32
	CB5011 + pVRASR-2	4	0.5
MAR-10	CB5013 (DS)	0.5	512
	CB5013 + pVRASR-2	6	256
MAR-11	CB1631 (DS)	0.5	32
	CB1631 + pVRASR-2	6	0.75
MAR-12	CB5048 (DS)	0.25	32
	CB5048 + pVRASR-2	2	2
MAR-13	CB5035 (DS)	0.25	512
	CB5035 + pVRASR-2	2	256

[a] OXA, oxacillin.

As mentioned before, the two-component regulator VraSR is actively involved in the regulation of cell wall stress induced by treatment with DAP (7, 35). To investigate the phenotypes associated with reduced susceptibility to DAP, we analyzed cell wall thickness in pair CB5011/CB5012 and derivative mutants. Electron microscopy analysis showed that DR CB5012 displayed a thicker cell wall (33.5 ± 1.2 nm) than DS CB5011 (Table 7). To determine the contribution of *mprF* and *vraSR* to cell thickness, mutants and complemented *mprF* and *vraSR* strains were analyzed. Inactivation of *mprF* in CB5012 (MAR-4) resulted in a significantly thinner cell wall (25.4 ± 1.1 nm) compared with that of CB5012 (33.2 ± 1.5 nm). Complementation with wild-type *mprF* (MAR-5) did not alter MAR-4 cell wall thickness; by contrast, complementation with mutated *mprF* (MAR-6) did restore it to the CB5012 original thickness, emphasizing the functional role of the *mprF* L826F mutation. On the other hand, CB5012 *vraSR* inactivation (MAR-7) also reduced cell wall thickness, an effect that was reversed by *vraSR* complementation (MAR-8). Thus, these results support the mechanistic involvement of both mutated

TABLE 7 Cell wall thickness of pair CB5011/CB5012 and mutant derivatives

Strain	Cell wall thickness (nm)	DAP MIC (μg/ml)	Relevant genotype and phenotype
CB5011	23.1 ± 1.1	0.5	DS
CB5012	33.2 ± 1.5[a]	4.0	DR
MAR-4	25.4 ± 1.1[b]	0.5	CB5012 + Δ*mprF*::*cat*
MAR-5	25.3 ± 1.3[b]	0.75	MAR-4 + pMPRF-1 (wild type)
MAR-6	35.5 ± 1.4	2.0	MAR-4 + pMPRF-2 (mutant)
MAR-7	24.5 ± 1.1[b]	0.25	CB5012 Δ*vraSR*::*cat*
MAR-8	31.3 ± 1.1	3.0	MAR-7 + pVRASR-2

[a] Significantly higher than DS CB5011 ($P < 0.01$).
[b] Significantly lower than DR CB5012 ($P < 0.01$).

mprF and increased expression of *vraSR* in DAP-resistant *S. aureus*. The data also suggest that the mutual presence of both genes is required to confer a maximal DAP-resistant phenotype.

DISCUSSION

Previous studies performed with *in vitro*-generated DAP-resistant strains demonstrated that four open reading frames representing three distinct proteins (i.e., MprF, an LPG synthetase; YycG, a sensor histidine kinase; and RpoB and RpoC, β and β' subunits of RNA polymerase) were implicated in DAP MIC increases (17). In support of these observations, several groups have reported an association between increased *S. aureus* DAP MICs and single point mutations in the *mprF* gene that are acquired during either *in vitro* or *in vivo* exposure to DAP (17, 20, 42). A gain-in-function mutation has been postulated to impact DAP nonsusceptibility via a charge-repulsive mechanism (25, 40). In a recent study performed on an isogenic set of clinical bloodstream *S. aureus* isolates, it was also observed that a DAP-nonsusceptible strain showed an increased expression of *mprF* associated with *mprF* point mutations (48). However, other investigations showed that neither the transcriptional profile of *mprF* nor the results of membrane phospholipid analyses were compatible with an *mprF* gain-in-function phenotype. In this case, the DAP-resistant phenotype appeared to be related to enhanced *dlt* expression coincident with an increased positive surface charge and reduced DAP binding (46). In the present study, which was conducted in isogenic DS/DR MRSA strains obtained from DAP-treated patients, we first attempted to determine whether similar events regarding *mprF* may account for the resistant phenotype. Although no changes in *mprF* expression levels were found, we determined the existence of point mutations that, as we were able to demonstrate, contributed to the mechanisms of DAP resistance. Furthermore, we found that, independently of their domain localization (i.e., putative synthase domain [CB5012] and N-terminal translocase domain [CB5036, CB183]), none of the identified *mprF* mutations produced significant changes in net cell surface charge in DR CB5012, CB5036, and CB183 strains compared to their corresponding susceptible DS counterparts, CB5011, CB5035, CB182, respectively. In agreement with these premises, the present group of strains displayed no changes in their susceptibility to cationic molecules such as gentamicin, indicating that surface charge may not represent the primary factor dictating DAP resistance in these strains. In support of these results, a recent study performed in *in vitro*-selected DAP-resistant *S. aureus* strains showed a reduction of cytochrome *c* binding and reduced cell membrane depolarization without associated *mprF* mutations (39), suggesting that in the absence of any changes in *mprF* or *dltA* expression or in the MprF sequence, additional loci may be involved in modulating the relative surface charge of *S. aureus* (39). Taking into account these observations, our results suggested that in addition to the L826F *mprF* mutation, other factors may be involved in DAP resistance. In fact, one of the most consistent observations among the different strains was that DAP resistance was accompanied by an increase in expression of the two-component regulator *vraSR*, which positively modulates cell wall biosynthesis (28). Previous observations showing that a change in the cell wall thickness is associated with DAP resistance (7) prompted us to look more closely at the function of *vraSR*. Furthermore, a number of genes differentially expressed when comparing DS and DR strains were well-known *vraSR*-regulated targets, including *pbp2* and *sgtB*. Our findings are in line with those of recent studies showing that DAP is able to induce the cell wall stress stimulon (16) and genes responsive to membrane depolarization in methicillin-susceptible *S. aureus* (35). Upregulation of *vraSR* has also been observed in *in vitro*-developed DAP-resistant *S. aureus* (7) and by transcriptome studies performed in *Bacillus subtilis*, where DAP strongly induced the transcription of the two-component system *liaRS*, a *vraSR* homolog (21). However, until now, no functional studies have been performed in clinical MRSA strains to address the VraSR contribution to the resistant phenotype. Our results clearly demonstrated that inactivation of *vraSR* in DR strains resulted in a significant decrease in DAP resistance. Moreover, overexpression of *vraSR* in DS strains significantly decreased susceptibility to DAP, indicating a functional role of increased *vraSR* expression as a factor associated with DAP resistance. The fact that a number of genes showing differential expression are under *vraSR* regulation further supports this notion. A group of *vraSR*-regulated genes was closely involved in cell wall synthesis, and our results consistently demonstrated that inactivation of *vraSR* in DR cells resulted in a thinner cell wall comparable to that of DS cells, suggesting that DAP resistance-mediated increased expression of *vraSR* may contribute to the DR phenotype by modulating components of cell wall synthesis. In the same context, results from microarray analyses showed upregulation of *vraF* and *vraG* in DR strains. These transporter proteins have been shown to be associated with vancomycin resistance as important components of activated cell wall peptidoglycan synthesis (33). The thickness of the cell wall has been reported to be associated with DAP-resistant strains (5, 7, 32), although not in all cases. Some of these studies were demonstrated in DAP-resistant strains that concomitantly displayed a vancomycin-intermediate *S. aureus* (VISA) phenotype, making it difficult to discern whether vancomycin can induce similar phenotypic perturbations as DAP in terms of cell wall thickness. In our investigation, DR strains did show a thickened cell wall with no parallel decrease in susceptibilities to vancomycin. Recently, it was also shown that the thickness of the cell wall in DAP-resistant strains was correlated with an increased capacity of these isolates to synthesize *d*-alanylate WTA, an effect mediated in part by the concomitant upregulation of WTA genes *tagA* and *dlt* (5). Converse to these observations, we did not observe changes in expression of these genes by either microarray analysis or real-time RT-PCR. One of the interesting aspects of our investigation is that the L826F mutation in the *mprF* gene had a mechanistic impact on cell wall thickness, as demonstrated by *mprF* inactivation and transcomplementation of either full-length wild-type or mutated

mprF in DR strains. These results suggested that although no direct effect at the cell net surface charge change was observed, the *mprF* L826F mutation contributed to cell wall thickness through a mechanism yet to be fully determined.

Similar to findings reported by other groups (32, 47), we observed a correlation between increased resistance to DAP and a concomitant decrease in oxacillin resistance, an effect that we found was not related to deletion or excision of SCC*mec*/*mecA*. We were able to reproduce this observation when *vraSR* was overexpressed in DS cells, further emphasizing the role of VraSR in the DR phenotype. In fact, deletion of the VraSR operon is known to decrease levels of resistance to most of its inducing antibiotics, including β-lactam antibiotics (13, 18, 28, 35). However, the precise mechanism by which increased susceptibility to β-lactams occurs in MRSA isolates with VraSR mutations/deletion remains unknown (24, 49). On the other hand, it may be plausible to speculate that the paradoxical effect observed when VraSR was overexpressed in the present group of strains could be related to the presence of *mprF* mutations, which in turn may affect VraSR sensing signaling toward cell wall-targeting antibiotics. Together, the present results suggest that DAP has an impact on the proper assembly of the staphylococcal cell wall, thereby affecting the cell response not only to DAP but also to oxacillin.

In summary, a key aspect of this study was the demonstration by genetic analysis and manipulation of the functional role played by *mprF* mutations. Furthermore, our results strongly suggest that the mechanisms and pathways underlying the *in vivo*-selected clinical daptomycin-resistant strains used in this study may be determined by the mutual cooperation between *mprF* and the two-component regulator VraSR through a mechanism that may involve regulation of genes related to cell wall synthesis and turnover.

ACKNOWLEDGMENTS

This research was supported by grants from Cubist Pharmaceuticals, Lexington, MA. Microarray studies were funded in part through a PFGRC-NIAID grant (to A.E.R.).

We acknowledge Gordon Archer for his input and discussions. Electron microscopy was performed at the VCU Department of Anatomy and Neurobiology Microscopy facility and at the Baylor College of Medicine, Houston, TX. We are very grateful to Keiichi Hiramatsu and Susan Boyle-Vavra for providing the KVR strain and pVRASR-2 plasmid, respectively. Special thanks go to Kathryn Stockbauer and Philip Randall, from the Office of Academic Development, TMHRI, for their assistance with manuscript editing.

REFERENCES

1. **Arbeit RD, Maki D, Tally FP, Campanaro E, Eisenstein BI.** 2004. The safety and efficacy of daptomycin for the treatment of complicated skin and skin-structure infections. Clin. Infect. Dis. **38**:1673–1681.
2. **Baltz RH.** 2009. Daptomycin: mechanisms of action and resistance, and biosynthetic engineering. Curr. Opin. Chem. Biol. **13**:144–151.
3. **Baltz RH, Miao V, Wrigley SK.** 2005. Natural products to drugs: daptomycin and related lipopeptide antibiotics. Nat. Prod. Rep. **22**:717–741.
4. **Bannerman TL, Hancock GA, Tenover FC, Miller JM.** 1995. Pulsed-field gel electrophoresis as a replacement for bacteriophage typing of *Staphylococcus aureus.* J. Clin. Microbiol. **33**:551–555.
5. **Bertsche U, et al.** 2011. Correlation of daptomycin resistance in a clinical *Staphylococcus aureus* strain with increased cell wall teichoic acid production and D-alanylation. Antimicrob. Agents Chemother. **55**:3922–3928.
6. **Boyle-Vavra S, Yin S, Daum RS.** 2006. The VraS/VraR two-component regulatory system required for oxacillin resistance in community-acquired methicillin-resistant *Staphylococcus aureus.* FEMS Microbiol. Lett. **262**:163–171.
7. **Camargo IL, Neoh HM, Cui L, Hiramatsu K.** 2008. Serial daptomycin selection generates daptomycin-nonsusceptible *Staphylococcus aureus* strains with a heterogeneous vancomycin-intermediate phenotype. Antimicrob. Agents Chemother. **52**:4289–4299.
8. **Chambers HF.** 1995. In vitro and in vivo antistaphylococcal activities of L-695,256, a carbapenem with high affinity for the penicillin-binding protein PBP 2a. Antimicrob. Agents Chemother. **39**:462–466.
9. **Chambers HF.** 2005. Community-associated MRSA—resistance and virulence converge. N. Engl. J. Med. **352**:1485–1487.
10. **Chambers HF, Archer G, Matsuhashi M.** 1989. Low-level methicillin resistance in strains of *Staphylococcus aureus.* Antimicrob. Agents Chemother. **33**:424–428.
11. **Cui L, Murakami H, Kuwahara-Arai K, Hanaki H, Hiramatsu K.** 2000. Contribution of a thickened cell wall and its glutamine nonamidated component to the vancomycin resistance expressed by *Staphylococcus aureus* Mu50. Antimicrob. Agents Chemother. **44**:2276–2285.
12. **Cuirolo A, Plata K, Rosato AE.** 2009. Development of homogeneous expression of resistance in methicillin-resistant *Staphylococcus aureus* clinical strains is functionally associated with a beta-lactam-mediated SOS response. J. Antimicrob. Chemother. **64**:37–45.
13. **Dengler V, Meier PS, Heusser R, Berger-Bachi B, McCallum N.** 2011. Induction kinetics of the Staphylococcus aureus cell wall stress stimulon in response to different cell wall active antibiotics. BMC Microbiol. **11**:16.
14. **Ernst CM, et al.** 2009. The bacterial defensin resistance protein MprF consists of separable domains for lipid lysinylation and antimicrobial peptide repulsion. PLoS Pathog. **5**:e1000660.
15. **Finan JE, Rosato AE, Dickinson TM, Ko D, Archer GL.** 2002. Conversion of oxacillin-resistant staphylococci from heterotypic to homotypic resistance expression. Antimicrob. Agents Chemother. **46**:24–30.
16. **Fischer A, et al.** 2011. Daptomycin resistance mechanisms in clinically derived Staphylococcus aureus strains assessed by a combined transcriptomics and proteomics approach. J. Antimicrob. Chemother. **66**: 1696–1711.
17. **Friedman L, Alder JD, Silverman JA.** 2006. Genetic changes that correlate with reduced susceptibility to daptomycin in *Staphylococcus aureus.* Antimicrob. Agents Chemother. **50**:2137–2145.
18. **Gardete S, Wu SW, Gill S, Tomasz A.** 2006. Role of VraSR in antibiotic resistance and antibiotic-induced stress response in *Staphylococcus aureus.* Antimicrob. Agents Chemother. **50**:3424–3434.
19. **Goldstein F, et al.** 2007. Identification and phenotypic characterization of a beta-lactam-dependent, methicillin-resistant Staphylococcus aureus strain. Antimicrob. Agents Chemother. **51**:2514–2522.
20. **Gqada Z, et al.** 2008. Clinical rationale for treatment of endocarditis caused by methicillin-susceptible *Staphylococcus aureus* developing nonsusceptibility to daptomycin. J. Clin. Microbiol. **46**:2471–2472.
21. **Hachmann AB, Angert ER, Helmann JD.** 2009. Genetic analysis of factors affecting susceptibility of *Bacillus subtilis* to daptomycin. Antimicrob. Agents Chemother. **53**:1598–1609.
22. **Ichihashi N, Kurokawa K, Matsuo M, Kaito C, Sekimizu K.** 2003. Inhibitory effects of basic or neutral phospholipid on acidic phospholipid-mediated dissociation of adenine nucleotide bound to DnaA protein, the initiator of chromosomal DNA replication. J. Biol. Chem. **278**: 28778–28786.
23. **Ito T, et al.** 2001. Structural comparison of three types of staphylococcal cassette chromosome mec integrated in the chromosome in methicillin-resistant *Staphylococcus aureus.* Antimicrob. Agents Chemother. **45**: 1323–1336.
24. **Jo DS, Montgomery CP, Yin S, Boyle-Vavra S, Daum RS.** 2011. Improved oxacillin treatment outcomes in experimental skin and lung infection by a methicillin-resistant *Staphylococcus aureus* isolate with a *vraSR* operon deletion. Antimicrob. Agents Chemother. **55**: 2818–2823.
25. **Jones T, et al.** 2008. Failures in clinical treatment of *Staphylococcus aureus* infection with daptomycin are associated with alterations in surface charge, membrane phospholipid asymmetry, and drug binding. Antimicrob. Agents Chemother. **52**:269–278.
26. **Julian K, et al.** 2007. Characterization of a daptomycin-nonsusceptible vancomycin-intermediate *Staphylococcus aureus* strain in a patient with endocarditis. Antimicrob. Agents Chemother. **51**:3445–3448.
27. **Kennedy AD, et al.** 2008. Epidemic community-associated methicillin-resistant *Staphylococcus aureus*: recent clonal expansion and diversification. Proc. Natl. Acad. Sci. U. S. A. **105**:1327–1332.

28. **Kuroda M, et al.** 2003. Two-component system VraSR positively modulates the regulation of cell-wall biosynthesis pathway in *Staphylococcus aureus.* Mol. Microbiol. **49**:807–821.
29. **Kuroda M, et al.** 2001. Whole genome sequencing of meticillin-resistant *Staphylococcus aureus.* Lancet **357**:1225–1240.
30. **Livak KJ, Schmittgen TD.** 2001. Analysis of relative gene expression data using real-time quantitative PCR and the 2(−delta delta C(T)) method. Methods **25**:402–408.
31. **Margolis PS, et al.** 2000. Peptide deformylase in *Staphylococcus aureus*: resistance to inhibition is mediated by mutations in the formyltransferase gene. Antimicrob. Agents Chemother. **44**:1825–1831.
32. **Mishra NN, et al.** 2009. Analysis of cell membrane characteristics of in vitro-selected daptomycin-resistant strains of methicillin-resistant *Staphylococcus aureus.* Antimicrob. Agents Chemother. **53**:2312–2318.
33. **Moe PC, Levin G, Blount P.** 2000. Correlating a protein structure with function of a bacterial mechanosensitive channel. J. Biol. Chem. **275**: 31121–31127.
34. **Mohedano ML, et al.** 2005. Evidence that the essential response regulator YycF in *Streptococcus pneumoniae* modulates expression of fatty acid biosynthesis genes and alters membrane composition. J. Bacteriol. **187**: 2357–2367.
35. **Muthaiyan A, Silverman JA, Jayaswal RK, Wilkinson BJ.** 2008. Transcriptional profiling reveals that daptomycin induces the *Staphylococcus aureus* cell wall stress stimulon and genes responsive to membrane depolarization. Antimicrob. Agents Chemother. **52**:980–990.
36. **NCCLS/CLSI.** 2007. Performance standards for antimicrobial disk susceptibility tests. Approved standard M2-A8, 8th ed. NCCLS/CLSI, Wayne, PA.
37. **Novick R.** 1967. Properties of a cryptic high-frequency transducing phage in Staphylococcus aureus. Virology **33**:155–166.
38. **Oliveira DC, de Lencastre H.** 2002. Multiplex PCR strategy for rapid identification of structural types and variants of the *mec* element in methicillin-resistant *Staphylococcus aureus.* Antimicrob. Agents Chemother. **46**:2155–2161.
39. **Patel D, et al.** 2011. Mechanisms of in-vitro-selected daptomycin-non-susceptibility in Staphylococcus aureus. Int. J. Antimicrob. Agents **38**: 442–446.
40. **Peschel A, et al.** 2001. *Staphylococcus aureus* resistance to human defensins and evasion of neutrophil killing via the novel virulence factor MprF is based on modification of membrane lipids with L-lysine. J. Exp. Med. **193**:1067–1076.
41. **Peschel A, et al.** 1999. Inactivation of the dlt operon in *Staphylococcus aureus* confers sensitivity to defensins, protegrins, and other antimicrobial peptides. J. Biol. Chem. **274**:8405–8410.
42. **Pillai SK, et al.** 2007. Daptomycin nonsusceptibility in *Staphylococcus aureus* with reduced vancomycin susceptibility is independent of alterations in MprF. Antimicrob. Agents Chemother. **51**:2223–2225.
43. **Rohrer S, Maki H, Berger-Bachi B.** 2003. What makes resistance to methicillin heterogeneous? J. Med. Microbiol. **52**:605–607.
44. **Rosato AE, Craig WA, Archer GL.** 2003. Quantitation of *mecA* transcription in oxacillin-resistant *Staphylococcus aureus* clinical isolates. J. Bacteriol. **185**:3446–3452.
45. **Tenover FC, et al.** 1995. Interpreting chromosomal DNA restriction patterns produced by pulsed-field gel electrophoresis: criteria for bacterial strain typing. J. Clin. Microbiol. **33**:2233–2239.
46. **Yang SJ, et al.** 2009. Enhanced expression of dltABCD is associated with the development of daptomycin nonsusceptibility in a clinical endocarditis isolate of *Staphylococcus aureus.* J. Infect. Dis. **200**:1916–1920.
47. **Yang SJ, et al.** 2010. Daptomycin-oxacillin combinations in treatment of experimental endocarditis caused by daptomycin-nonsusceptible strains of methicillin-resistant *Staphylococcus aureus* with evolving oxacillin susceptibility (the "seesaw effect"). Antimicrob. Agents Chemother. **54**: 3161–3169.
48. **Yang SJ, et al.** 2009. Regulation of *mprF* in daptomycin-nonsusceptible *Staphylococcus aureus* strains. Antimicrob. Agents Chemother. **53**: 2636–2637.
49. **Yin S, Daum RS, Boyle-Vavra S.** 2006. VraSR two-component regulatory system and its role in induction of pbp2 and vraSR expression by cell wall antimicrobials in *Staphylococcus aureus.* Antimicrob. Agents Chemother. **50**:336–343.